HHS Public Access

Author manuscript

Neuroendocrinology. Author manuscript; available in PMC 2021 January 01.

Published in final edited form as:

Neuroendocrinology. 2020 ; 110(1-2): 105–118. doi:10.1159/000501560.

Estradiol Protects Neuropeptide Y/Agouti-related Peptide Neurons against Insulin Resistance in Females

Jian Qiu[1,*], **Martha A. Bosch**[1], **Chunguang Zhang**[1], **Oline K. Rønnekleiv**[1,2], **Martin J. Kelly**[1,2,*]

[1]Department of Physiology and Pharmacology, Oregon Health & Science University, Portland, Oregon, USA

[2]Division of Neuroscience, National Primate Research Center, Oregon Health & Science University, Beaverton, Oregon, USA

Abstract

With obesity men exhibit a higher incidence of metabolic syndrome than women in early adult life, but this sex advantage wanes in postmenopausal women. A key diagnostic of the metabolic syndrome is insulin resistance in both peripheral tissues and brain, especially in the hypothalamus. Since the anorexigenic hormone 17β-estradiol (E_2) regulates food intake in part by inhibiting the excitability of the hypothalamic neuropeptide Y/agouti-related peptide (NPY/AgRP) neurons, we hypothesized that E_2 would protect against insulin resistance in NPY/AgRP neurons with diet-induced obesity (DIO). Therefore, we did whole-cell recordings and single cell qPCR in arcuate NPY^{GFP} neurons from both female and male mice to test the efficacy of insulin with DIO. The resting membrane potential and input resistance of NPY/AgRP neurons was significantly increased in DIO versus control-diet fed males. Most notably, the efficacy of insulin to activate K_{ATP} channels in NPY/AgRP neurons was significantly attenuated, although the K_{ATP} channel opener diazoxide was fully effective in NPY/AgRP neurons from DIO males, indicating that the K_{ATP} channels were expressed and functional. In contrast, insulin was fully efficacious to activate K_{ATP} channels in DIO females, and the response was reversed by the K_{ATP} channel blocker tolbutamide. However, the ability of insulin to activate K_{ATP} channels was abrogated with ovariectomy but fully restored with E_2 replacement. The insulin resistance in obese males was likely mediated by an increase in suppressor of cytokine signaling-3 (SOCS-3), protein tyrosine phosphatase B (PTP1B) and T cell protein tyrosine phosphatase (TCPTP) activity since the expression of all three mRNAs were upregulated in the obese males but not in females. As proof of principle, pre-incubation of hypothalamic slices from DIO males with the PTP1B/TCPTP inhibitor CX08005 completely rescued the effects of insulin. Therefore, E_2 protects NPY/AgRP neurons in females against insulin resistance through, at least in part, attenuating phosphatase

[*]Corresponding Author: Martin J. Kelly and Jian Qiu, Department of Physiology and Pharmacology, Oregon Health & Science University, 3181 Southwest Sam Jackson Park Road, Portland, Oregon, 97239, USA, Tel: 503-494-5833, Fax: 503-494-4352, kellym@ohsu.edu; qiuj@ohsu.edu.

Author Contributions: J.Q. and C.G.Z. performed and analyzed the electrophysiology experiments. M.A.B. did the single-cell harvesting and quantitative PCR analysis of the harvested cells. M.J.K., O.K.R. and J.Q. designed the experiments, analyzed the data, and wrote the manuscript. We thank Ashley M. Connors and Uyen-Vy Navarro for technical assistance with mouse body weight and body composition measurements.

The authors have no conflicts of interest to declare.

activity. The neuroprotective effects of E_2 may explain sex differences in the expression of metabolic syndrome that disappears with the loss of E_2 in aging.

Keywords

Estradiol; Hypothalamus; NPY/AgRP; Obesity; Insulin Resistance

Introduction

At the center of the regulation of energy homeostasis, and hence the central feedback of insulin, are the anorexigenic proopiomelanocortin (POMC) and orexigenic neuropeptide Y/agouti-related peptide (NPY/AgRP) neurons in the hypothalamic arcuate nucleus (ARH). These two neuronal populations are adjacent to the median eminence and hence are strategically located for monitoring hormones and nutrients and transmitting homeostatic signals to other areas [1]. Also, the NPY/AgRP neurons in particular are involved in integrating anticipatory sensory cues to generate appropriate feeding behavior [2]. Hence, optogenetic and pharmacogenetic stimulation of NPY/AgRP neurons rapidly increases food consumption [3, 4], whereas stimulation of POMC neurons attenuates food intake [3, 5]. NPY/AgRP and POMC neurons are also the major CNS targets of insulin and leptin actions [6–10].

In an *ex vivo* hypothalamic slice preparation, insulin hyperpolarizes NPY/AgRP neurons via activation of K_{ATP} channels, whereas it depolarizes POMC neurons via activation of canonical transient receptor potential (TRPC5) channels, activities that are consistent with the anorexigenic effects of insulin [9, 11]. Insulin infused into the third ventricle *(icv)* decreases food intake in guinea pigs [9], mice [12, 13] and rats [14], which correlates with alterations in energy expenditure as exhibited by increases in O_2 consumption, CO_2 production and metabolic heat production [9]. Also, *icv* insulin lowers blood glucose and suppresses hepatic glucose production (gluconeogenesis) [15]. Selective deletion of the insulin receptor in NPY/AgRP neurons abrogates the ability of insulin to hyperpolarize and inhibit NPY/AgRP neurons and subsequently to lower hepatic glucose production [16]. Re-expression of the insulin receptor in NPY/AgRP neurons (and liver and pancreas) rescues the ability of insulin to control hepatic gluconeogenesis [17]. In addition, *icv* insulin reduces lipolysis and promotes lipogenesis in adipocytes through a decrease in sympathetic tone to white adipose tissue [9, 18]. Therefore, insulin signaling in the hypothalamus plays a major role in controlling hepatic glucose production.

Spanswick and colleagues first described the efficacy of insulin to hyperpolarize hypothalamic arcuate neurons in the rat, presumably only males, in a phosphoinositide 3-kinase (PI3K)-dependent manner [19]. In later studies using transgenic mice, it was shown that insulin specifically hyperpolarizes and inhibits the activity of both male and female NPY/AgRP neurons via a PI3K signaling pathway [9, 15, 16, 20, 21]. A more recent study found that selective deletion of the PI3K catalytic subunits p110α and p110β in NPY/AgRP neurons of male mice eliminated the direct response to insulin in a slice preparation, and male mice exhibited weight gain, both an increase in fat and lean mass, on a regular chow

diet [21]. PI3K generates phosphatidylinositol-3,4,5-triphosphate (PIP_3) from phosphatidylinositol 3,4-diphosphate (PIP_2), which stimulates phospholipase C (PLC) and protein kinase B (Akt) [9, 22–24], but it is the generation of PIP_3 from PIP_2 (removal of PIP_2 from the membrane) that facilitates the K_{ATP} channel opening [25].

A key "molecular switch" for controlling insulin receptor coupling to downstream effector systems in NPY/AgRP neurons appears to be T-cell protein tyrosine phosphatase (TCPTP) activity. Fasting increases TCPTP expression in the mediobasal hypothalamus, whereas feeding represses TCPTP expression and promotes its degradation in male mice [26]. The postprandial decrease in TCPTP expression facilitates insulin receptor coupling to K_{ATP} channel activation, which inhibits neuronal activity [26] that ultimately affects whole-body glucose metabolism [27]. Moreover, selective deletion of the gene encoding TCPTP *(Pnpt2)* in NPY/AgRP neurons enhances insulin receptor signaling in NPY/AgRP neurons and consequently whole-body insulin sensitivity and glucose homeostasis in male mice [27], all of which are thought to be a direct consequence of the activation of K_{ATP} channels in NPY/AgRP neurons [10, 16, 28], which is the focus of the present study.

Insulin resistance is at the core of the metabolic syndrome and there is a sex difference in the expression of insulin resistance in adults. Neurons, similar to any cell, develop hyperinsulinemia-induced insulin resistance, which results in severe injury to the nervous system as seen in diabetic neuropathies [29]. Males exhibit a higher incidence of metabolic syndrome than women in early adult life, but this sex difference diminishes abruptly in hypoestrogenic states [30, 31]. We discovered that POMC neurons from diet-induce obese male rodents were refractory to the actions of insulin—*i.e.*, the activation of canonical transient receptor potential 5 (TRPC5) channels was completely abrogated in obese males [11]. In contrast, insulin was fully efficacious in obese, reproductively active females. However, ovariectomy eliminated this protection, but 17β-estradiol (E_2) rescued the insulin response such that E_2 replacement reinstated the insulin effects. Since NPY/AgRP neurons are also a critical player and maybe even more important for control of hepatic glucose production [16], we hypothesized that E_2 would protect against insulin resistance with diet-induced obesity in NPY/AgRP neurons, similar to POMC neurons.

Materials and Methods

Animals and treatments

All animal procedures described in this study were performed in accordance with institutional guidelines based on National Institutes of Health standards and approved by the Institutional Animal Care and Use Committee at Oregon Health & Science University.

Mice

For the electrophysiology and single-cell reverse transcription (RT) polymerase chain reaction (PCR) experiments, female and male *Npy*^{GFP} transgenic mice (provided by Dr. Brad Lowell, Harvard University, Cambridge, MA) [32] were selectively bred in-house and maintained under controlled temperature (25°C) and photoperiod conditions (lights on at 6 AM and off at 6 PM) with food and water ad libitum. We used a well-established, diet-

induced obese mouse model to do cellular studies on NPY/AgRP neurons [11, 33, 34]. *Npy*^{GFP} mice were put on a high-fat diet (HFD; 45% kcal from fat; Research Diets, New Brunswick, NJ; D12451) starting at 3 weeks of age for 10 weeks to induce diet-induced obesity (DIO). A control group of mice received normal grain-based chow (5L0D; Laboratory Diets, St. Louis, MO). After at least 10 weeks on their diets (>13 weeks of age), we prepared coronal slices from both groups of mice and did whole-cell voltage clamp recording from *Npy*^{GFP} (NPY/AgRP) neurons. In females, the estrous cycle was monitored daily based on vaginal cell cytology for at least 2 weeks before using the animals for electrophysiological experiments on proestrus. Other animals were ovariectomized (OVX) one week before the electrophysiology experiments and treated with 17β-estradiol benzoate (EB) as previously described [11]. High circulating (proestrous) levels of E_2 were verified by the uterine weights (> 90 mg) at the time of hypothalamic slice preparation. Mice were housed individually, and body weight and food intake measurements were determined every 2 weeks. Food intake was determined as grams of diet consumed per day. The body composition was assessed with an EchoMRI Whole Body Composition Analyzer (Echo Medical Systems, Houston, TX).

Glucose tolerance test (GTT).—All mice were weaned at 3 weeks of age and given either a control diet or HFD as described above. Age-matched control and DIO mice were fasted for 15-h and baseline glucose levels measured with the aid of an Accu-Check Advantage blood glucose meter (Roach) using blood collected from the tail vein. Mice were injected intraperitoneally with glucose (1 mg/g lean mass as determined by MRI) in sterile PBS and blood glucose levels were measured 15, 30, 60, 90, and 120 min after injection. Glucose clearance (Area under the Curve, AUC) was calculated based on the glucose baseline levels at 0 min [32].

Visualized whole-cell patch recording

Whole-cell current clamp and voltage clamp recordings were made from Npy^{GFP} neurons as previously described [35]. Coronal arcuate slices (250 μm) were prepared from males and females as previously described [9]. Whole-cell patch recordings were made from *Npy*^{GFP} neurons using an Olympus BX51 W1 fixed-stage scope outfitted with epifluorescence and infrared differential interference contrast video microscopy. Patch pipettes (A-M Systems; 1.5-mm outer diameter borosilicate glass; World Precision Instruments, Sarasota, FL) were pulled on a Brown/Flaming puller (P-97; Sutter Instrument, Novato, CA) and filled with the following internal solution: 128 mM potassium gluconate, 10 mM NaCl, 1 mM $MgCl_2$, 11 mM EGTA, 10 mM HEPES, 3 mM adenosine triphosphate, and 0.25 mM GTP adjusted to pH 7.3 with KOH (295 mOsm). Pipette resistances ranged from 3.5 to 4 MΩ. In whole-cell configuration, access resistance was less than 20 MΩ; the access resistance was 80% compensated. The input resistance was calculated by measuring the slope of the current-voltage (I-V) relationship curve between −70 and −50 mV. Standard whole-cell patch recording procedures and pharmacological testing were performed as previously described [11]. Electrophysiological signals were digitized with a Digidata 1322A (Axon Instruments), and the data were analyzed using p-Clamp software (Molecular Devices, Foster City, CA). The liquid junction potential was corrected for all data analysis. I-V relationships of the

insulin-generated currents were constructed by voltage ramps from −120 to 0 mV from a holding potential of −60 mV.

Electrophysiological solutions/drugs

A standard artificial cerebrospinal fluid (aCSF) was used [11]. All drugs were purchased from Calbiochem (San Diego, CA) unless otherwise specified. Purified guinea pig insulin was purchased from Dr. Al Parlow (Harbor-UCLA Medical Center, Torrance, CA) through the National Hormone and Peptide Program. The hyperpolarizing (outward current) responses to purified guinea pig insulin were exactly the same as what we have published for bovine (Sigma-Aldrich I-1882) and human recombinant (Sigma-Aldrich I-9278) insulin [9]. The responses to insulin were measured when the outward current reached a steady state in 2–15 min, at which time the steady-state current was averaged over a 30 second time period. 17β-estradiol benzoate (EB) was purchased from Steraloids (Newport, RI) and dissolved in ethanol before oil dissolution. Diazoxide (7-chloro-3-methyl-2H-1,2,4-benzo-thiadiazin 1,1-dioxide) and tolbutamide (Sigma, St. Louis, MO) were dissolved in dimethylsulfoxide (DMSO) to a stock concentration of 300 mM and 100 mM, respectively. CX08005 (Sigma-Aldrich) was dissolved in DMSO to stock concentration of 20 mM. Aliquots of the stock solutions were stored as appropriate until needed.

Cell harvesting of dispersed Npy^{GFP} neurons and qPCR

Intact males and females were fed grain-based control diet or high-fat diet as described above. After ~ 10 weeks on their respective diets, all the females were ovariectomized and treated 5 days later with a low dose (0.25 μg) of EB and a high dose (1.50 μg) of EB on day 6 before using for experiments on day 7 [36]. Cell harvesting and qPCR were conducted as previously described [37, 38]. The ARH was microdissected from basal hypothalamic coronal slices obtained from control, EB-treated OVX females and DIO, EB-treated OVX females and control and DIO male Npy^{GFP} mice (n = 5 to 6 animals/group). The Npy^{GFP} dispersed cells were visualized, patched, and then harvested (10 cells/tube) as described previously [38]. Briefly, the tissue was incubated in protease (1 mg/mL in oxygenated artificial cerebrospinal fluid, aCSF for 15 minutes at 37°C) or papain (7 mg/ml in oxygenated aCSF for 40 minutes at 30°C) and washed 4 times in low Ca^{2+} aCSF (and 2 times in aCSF). Gentle trituration with Pasteur pipettes of decreasing size were used to disperse the neurons onto a glass-bottom dish. We designed a glass-bottom 60 mm dish to increase the surface area of the plate to allow greater segregation among cells. The healthy cells settled on the glass bottom dish after approximately 15 to 20 minutes, at which time the aCSF was removed and fresh aCSF was added to the plate. Throughout the dispersion and harvesting procedure, a constant flow (2 mL/min) of oxygenated aCSF circulated into the plate while the effluent circulated out using a peristaltic pump. The aCSF flow helped ensure fresh, oxygenated media was reaching the cells and assisted in clearing out unhealthy cells and debris from the trituration. The cells harvested were those observed to be fully intact, with one to three processes and a smooth cell membrane. The cells were harvested using the XenoWorks Microinjector System (Sutter Instrument, Novato, CA). This microinjector system provides negative pressure in the pipette, which, together with the fine and gentle control of the suction, allows each cell to be drawn into the pipette essentially without fluid. Cells were harvested as pools of 10 individual cells/tube.

Primers for the genes that encode for SOCS-3 *(Socs3)*, TCPTP *(Ptpn2)*, PTP1B *(Ptpn1)*, Navβ2 *(Scn2b)*, PI3K p110β *(Pi3kcb)*, and glyceraldehyde 3-phosphate dehydrogenase *(Gapdh)* were designed using Clone Manager software (Sci Ed Software, Denver, CO) (Table 1). Socs3, Pi3K p110β, Navβ2, and GAPDH primers have been previously published. [11, 39]. Primers cross at least one intron-exon boundary and are optimized as previously described using the Power SYBR Green method [37]. Given that the *Socs3* gene only expresses one intron, which made it difficult to design efficient primers for PCR quantification, we designed a primer pair that did not cross exon-intron boundaries. Therefore, to avoid amplifying genomic DNA, the harvested neuronal pools used to measure *Socs3* were treated with DNase I (1 U/mg DNA; Invitrogen, Grand Island, NY) at 10^{-3} U for 10 minutes and heat denatured (65°C) for 5 minutes prior to reverse transcription as previously described [11]. Controls included neuronal pools reacted without RT, hypothalamic RNA reacted with RT and without RT, and water blanks. Primers for qPCR were further tested for efficiency ($E = 10^{(-1/m)} - 1$, where m is the slope [40]), which varied from 96% to 100% (Table 1). qPCR was performed on a Quantstudio 7 Flex Real-Time PCR System (Life Technologies, Grand Island, NY) using Power SYBR Green Master Mix (Life Technologies) according to established protocols [37]. The comparative cycle threshold ($2^{-\Delta\Delta CT}$) method was used to determine fold change from duplicate samples of 4 μL for the target genes *Socs3, Ptpn2, Ptpn1, Scn2b, Pi3kcb*, and 2 μL for the reference gene *Gapdh* [41].

To determine the relative expression levels of target genes in *Npy*^{GFP} neurons obtained from control grain-fed animals compared with DIO animals, four pools (10 cells/pool) from each of 5-6 animals were used. The mean ΔCT from the grain-fed samples were used as the calibrator. The data were expressed as the change in gene expression normalized to the reference gene *Gapdh* and relative to the calibrator, and the mean and standard error of the mean were calculated and used for statistical analysis [37].

Results

NPY/AgRP neurons in obese males are insulin resistant

The average food intake (kcal/d) between control diet and HFD male or female Npy^{GFP} mice was not significantly different (unpaired t-test for males, $t_{(18)} = 1.691$; $p = 0.1081$; Controls: 17.8 ± 1.2 kcal/d, n = 8 versus DIO males: 15.7 ± 0.5 kcal/d, n = 12; unpaired t-test for females, $t_{(20)} = 0.0084$; $p = 0.9934$; Controls: 14.4 ± 0.8 kcal/d, n = 9 versus DIO females: 14.4 ± 0.3 kcal/d, n = 13). However, the total body weight of DIO male and female *Npy*^{GFP} mice was significantly greater than control diet mice by week 4 or 2, respectively (Fig. 1A and 1E). The average lean mass of DIO male and female *Npy*^{GFP} mice was significantly greater than mice fed a control diet by week 4 (DIO males: 17.8 ± 0.4 g; control males: 15.2 ± 0.3 g) (Fig. 1B) or week 2 (DIO females: 12.8 ± 0.3 g; control females: 11.7 ± 0.3 g) (Fig. 1F). More importantly, the average fat mass of DIO male *Npy*^{GFP} mice was significantly greater than control diet mice by week 6 (DIO males: 4.4 ± 0.4 g; control males: 2.1 ± 0.1 g) (Fig. 1C), whereas the average fat mass of DIO female *Npy*^{GFP} mice was significantly greater than control diet mice by week 2 (DIO females: 2.8 ± 0.2 g; control females: 1.4 ± 0.1 g) (Fig. 1G). After 10 weeks on their diets (13 weeks of

age), the fat mass data presented as percentage of total body weight were significantly different between controls and DIO groups (controls: 8.7 ± 0.6 %, n = 4 versus DIO males: 24.1 ± 2.6 %, n = 5, unpaired t-test, $t_{(7)} = 1.158$; $p = 0.0015$; controls: 12.0 ± 0.9 %, n = 8 versus DIO females:20.7 ± 1.6 %, n = 12, unpaired t-test, $t_{(18)} = 4.231$; $p = 0.0005$). Moreover, both DIO males and females had a significantly different glucose clearance rate than their age-matched controls (Figs. 1D, H: AUC: DIO males: 25,265 ± 984 mg/dL × min, n = 12 versus control males: 21,870 ± 365 mg/dL × min, n = 9, $t_{(19)} = 2.861$, $p = 0.0100$; DIO females: 21,425 ± 873 mg/dL × min, n = 12 versus control females: 16,730 ± 1,387 mg/dL × min, n = 8, $t_{(18)} = 3.023$, $p = 0.0073$).

Subsequently, we prepared hypothalamic slices from the DIO *Npy*^{GFP} mice after 10 weeks on their diets and did whole-cell current and voltage clamp recordings from NPY/AgRP neurons in male mice using established protocols to determine the efficacy of insulin to hyperpolarize NPY neurons [9]. DIO male mice were ~34% heavier than controls at the time that they were euthanized for electrophysiology studies (34.1 ± 3.0 g, n = 7 vs 25.5 ± 0.5 g, n = 14, respectively, unpaired two-tailed t test, $t_{(19)} = 4.016$, p = 0.0007) and had deposited ~4.6 times as much total body fat. Consistent with the EchoMRI data, the perigonadal fat pad in DIO males was significantly heavier as compared with the control diet males (1573 ± 267 mg, n = 6 vs 339 ± 24 mg, n=14, unpaired t-test, t(18) = 7.163, p < 0.0001). For the male NPY/AgRP neurons, there was no difference in the membrane capacitance (DIO males: 14.7 ± 0.7 pF, n = 14 versus controls: 14.8 ± 1.0 pF, n = 14; unpaired *t*-test, $t_{(26)} = 0.05851$, $p = 0.9538$), but there was a significant difference in the resting membrane potential (DIO males: −75.6 ± 2.1 mV, n = 38 versus controls: −63.6 ± 1.9 mV, n = 36; unpaired t-test, $t_{(72)} = 2.243$, p < 0.0003) and input resistance (DIO males: 2.0 ± 0.2 GΩ, n = 38 versus controls: 1.5 ± 0.1 GΩ, n = 36; unpaired t-test, $t_{(72)} = 2.343$, p = 0.0219) between the two groups, suggesting that the hyperpolarized resting membrane potential in DIO males could not have resulted from the opening of K^+ channels (including K_{ATP} channels). As previously reported, we documented that NPY/AgRP neurons are hyperpolarized/inhibited by nanomolar concentrations of purified insulin through activation of K_{ATP} channels that generates an outward current with a reversal of −87.7 ± 4.3 mV (n = 3) and an inwardly-rectifying current-voltage plot (I/V) [9]. Therefore, we used voltage-clamp recordings in both control and DIO animals to assess the response to insulin. We also generated I/V's before and after insulin to verify the underlying conductance (Fig. 2B, D). As hypothesized, there was a significant difference in the steady-state response (outward current) to 20 nM insulin (DIO males: 3.2 ± 1.1 pA, n = 14 versus controls: 9.5 ± 1.1 pA, n = 14, unpaired t-test, $t_{(26)} = 3.989$, p = 0.0005) (Figs. 2A–D and G). Therefore, insulin appeared to be less efficacious in DIO males to activate K_{ATP} channels.

Diazoxide has been shown to stimulate the opening of K_{ATP} channels [42]. Therefore, we tested diazoxide in NPY/AgRP neurons from DIO males to assess whether the K_{ATP} channel conductance was diminished in the DIO state. Diazoxide (300 μM) was able to fully activate the channels (18.4 ± 2.4 pA, n = 7 in control males and 16.8 ± 2.8 pA, n = 6 in DIO males), and the I/V revealed that outward current generated by diazoxide matched the effects of insulin in the controls with a reversal potential of −90 ± 2.6 mV (n = 6), indicative of activation of K_{ATP} channels (Fig. 2E, F, H). Therefore, it appeared that the K_{ATP} channels

were not downregulated in DIO males, but instead, there was an uncoupling of InsRs from channel activation.

NPY/AgRP neurons in obese, proestrous females maintain insulin sensitivity

To test for a potential sex difference in the response to insulin with DIO after 10 weeks, we did whole-cell current and voltage clamp recordings from NPY/AgRP neurons from DIO female *Npy*^{GFP} mice. The DIO female mice were ~12.5% heavier than controls at the time that they were euthanized for electrophysiology studies (24.3 ± 1.6 g, n = 4, vs 21.6 ± 0.5 g, n = 10, respectively, unpaired t-test, $t_{(12)}$ =2.254, p = 0.0437) and deposited ~3 times as much total body fat. The uterine weights between control and DIO females at the proestrous stage were not significantly different (controls: 106.3 ± 16.9 mg, n = 5 versus DIO females: 100.3 ± 6.1 mg, n = 4, unpaired t-test, $t_{(7)}$ = 0.3007; p = 0.7724). Consistent with the EchoMRI data, the perigonadal fat pad was significantly heavier in the DIO females compared with controls (895 ± 137 mg, n = 4 versus 171 ± 25 mg, n = 6, unpaired t-test, $t_{(8)}$ = 6.396, p = 0.0002). In contrast to males, there was no difference in the resting membrane potential (DIO females: −65.1 ± 1.5 mV, n = 13 versus controls: −64.2 ± 1.3 mV, n = 23, unpaired t-test, $t_{(34)}$ = 0.4120, p = 0.6829) or input resistance (DIO females: 1.4 ± 0.1 GΩ, n = 41 versus controls: 1.2 ± 0.1 GΩ, n = 24, unpaired t-test, $t_{(63)}$ = 1.340, p = 0.185) or membrane capacitance (controls: 14.9 ± 0.6 pF, n = 24 versus DIO females: 13.9 ± 0.6 pF, n = 41, unpaired t-test, $t_{(63)}$ = 1.158; p = 0.2514) between the two groups. Again, we used sensitive voltage-clamp recordings to access the effects of insulin. Also in contrast to the males, the steady-state response (outward current) to 20 nM insulin was not attenuated in DIO females (DIO females: 8.6 ± 1.8 pA, n = 11, controls:8.7 ± 2.3 pA, n = 8) (Fig. 3A and 3C, summarized in Fig. 3E). The insulin-induced outward current reversed at −88.6 ± 1.9 mV (n=7) in controls and −87.0 ± 3.1 mV (n = 4) in DIO females (Fig. 3B, D), and was antagonized by the K_{ATP} channel blocker tolbutamide (Fig. 3A and 3C). The diazoxide-induced outward current was also not different between control and DIO females (summarized in Fig. 3F). Therefore, we were confident that the insulin response was mediated by the opening of K_{ATP} channels. Hence, there was no attenuation of the insulin response (*i.e.,* K_{ATP} channel activation) in NPY/AgRP neurons from DIO proestrous females, which would indicate that there is a sex difference in the development of insulin resistance by NPY/AgRP neurons in obesity.

17β-estradiol protects NPY/AgRP neurons against insulin resistance

To explore the role of the gonadal steroids in preserving the insulin response in DIO females, we ovariectomized another cohort of female *Npy*^{GFP} mice that had been maintained on an HFD for 10 weeks. One week following ovariectomy, we gave one group (n = 5) an estradiol benzoate treatment regimen that yielded proestrous serum levels of E_2 [37] and treated the other group with the oil vehicle (n = 3). In contrast to insulin response in OVX females (n= 3) fed a control diet in which there was a significant insulin-mediated current (14.1 ± 2.7 pA, n = 7 neurons) (Fig. 4A, D), NPY/AgRP neurons from OVX, DIO females were completely refractory to the effects of insulin (*i.e.,* there was essentially no outward current, 1.4 ± 0.9 pA, n = 9; Fig. 4B, D). In contrast, NPY/AgRP neurons from EB-treated, OVX DIO females maintained their sensitivity to insulin (*i.e.,* insulin induced a robust outward current, 9.6 ± 2.2 pA, n = 12; Fig. 4C, D). Therefore, in the absence of E_2, there

appears to be an uncoupling of insulin receptor from activating K_{ATP} channels in obese females, but the insulin response is rescued with E_2 replacement.

Suppressor of cytokine signaling-3 (SOCS-3), protein tyrosine phosphatase 1B (PTP1B) and T cell protein tyrosine phosphatase (TCPTP) are differentially regulated in obesity

Leptin upregulates the expression of SOCS-3 in numerous cell types including NPY/AgRP neurons, and SOCS-3 negatively regulates leptin signaling by inhibiting the coupling of the leptin receptor (LRb) to the Janus kinase (JAK2) signaling pathway and may also negatively regulate insulin signaling [43]. Indeed, mice fed a high fat diet develop glucose intolerance, which is markedly improved by inactivating the *Socs3* gene in POMC neurons [44]. Since we previously found that a high fat diet upregulates *Socs3* mRNA expression in POMC neurons [11], we hypothesized that *Socs3* mRNA expression may be up-regulated in NPY/AgRP neurons from insulin-resistant, DIO males but not in insulin-responsive, DIO females. In addition, recent experimental evidence has also implicated tyrosine phosphatases, particularly TCPTP, in regulating leptin and insulin signaling in POMC and NPY/AgRP neurons (see [45] for review). Specifically, TCPTP dephosphorylates tyrosine-phosphorylated substrates such as the insulin receptor to antagonize insulin signaling. Therefore, there were compelling reasons to measure both *Socs3* and *Ptpn2* mRNA expression in the NPY/AgRP neurons since both would severely impede insulin signaling in the obese state. Both male and female mice were fed control grain-based diet or high-fat diet as described above and after 10 weeks NPY ^{GFP} neurons were dispersed and harvested as previously described [11], and *Socs3* and *Ptpn2* were measured using qPCR (see Methods). As predicted, both *Socs3* and *Ptpn2* mRNA expression were increased by approximately 40 % in NPY/AgRP neurons from DIO males as compared to the control diet-fed males (Fig. 5A, B). In contrast, neither *Socs3* nor *Ptpn2* mRNA expression were significantly altered in NPY/AgRP neurons from EB-treated, ovariectomized DIO females as compared to EB-treated control females (Fig. 5E, F), indicating that EB prevented the increase in both *Socs3* and *Ptpn2* mRNA expression with DIO, thereby maintaining insulin signaling in female NPY/AgRP neurons. Based on conditional deletion of PI3K p110β and/or p110α catalytic subunits in NPY/AgRP neurons of male mice, the PI3K signaling pathway has been shown to play a critical role in NPY/AgRP neuronal regulation of energy balance and glucose homeostasis [21, 46]. Therefore, we measured PI3K p110β (*Pi3kcb*) transcripts in control and DIO males and found no difference in the mRNA expression between the two groups (control diet mRNA relative expression: 1.12 ± 0.14, n=5; DIO mRNA relative expression: 1.18 ± 0.10, n=6), indicating that the PI3K pathway was functioning normally. A recent publication has also implicated protein tyrosine phosphatase 1B (*Ptpn1*) in attenuating insulin signaling in NPY/AgRP neurons in hyperleptinemic states [47] and as such we measured this phosphatase expression in both males and females. Indeed, Ptpn1 mRNA expression was increased by ~50 % in DIO males but not in DIO, EB-treated, OVX females (Fig. 5C, G). As a “negative” transcript control, we also measure the sodium channel β2 subunit (*Scn2b*) that we have published is regulated by E_2 in kisspeptin neurons [39] and found that the channel subunit expression was unaltered in both DIO males and females versus their control diet-fed counterparts (Fig. 5D, H). As proof of principle, we prepared slices from DIO males after 10 weeks on their diet and pre-incubated the slices in vehicle or the mixed PTP1B/TCPTP inhibitor CX08005 (20 μM for 4 h), respectively [48], and then

NPY^{GFP} neurons were patched and tested for their response to bath perfused insulin. To our surprise not only was insulin effective, but it was fully efficacious to hyperpolarize and inhibit firing of NPY/AgRP neurons versus the non-treated slices, and the effects were fully reversed by K_{ATP} channel blocker tolbutamide (Fig. 6C–D versus A–B, summarized in 6E). Therefore, the phosphatase activity appears to be a molecular switch for dictating the insulin response in DIO males, and EB-treated females are protected against changes in PTP1B/TCPTP expression with DIO.

Discussion

Although obesity produces dramatic alterations in metabolic phenotype in both males and females, E_2 was able to protect females from the development of hypothalamic insulin resistance. Insulin was fully efficacious to activate K_{ATP} channels and hyperpolarize NPY/AgRP neurons in DIO, proestrous and EB-treated, ovariectomized females but not in DIO, ovariectomized female or in male mice. Treating ovariectomized females with an estradiol regime that mimicked proestrous serum levels of E_2 fully restored the electrophysiological response to insulin in NPY/AgRP neurons. Also, E_2 prevented the increase in *Socs3, Ptpn1* and *Ptpn2* mRNA expression with DIO, all of which are known to inhibit the coupling of the insulin receptor with its downstream signaling cascades [44] [45] [49]. Therefore, the present studies have identified a sex difference in the development of insulin resistance in NPY/AgRP neurons that involves insulin receptor uncoupling from downstream signaling cascades that ultimately activate K_{ATP} channels in these orexigenic hypothalamic neurons.

In obese males but not in obese females the mRNA expression of *Socs3, Ptpn1* and *Ptpn2* increased by 40–50% in NPY/AgRP neurons, rendering males but not the females refractory to the effects of insulin; and in our guinea pig model of obesity, males but not females were resistant to the effects of *icv* insulin [38]. SOCS-3 is known to inhibit the tyrosine kinase activity of the insulin receptor and its interaction with insulin receptor substrate (IRS) proteins; SOCS-3 also targets IRS proteins toward degradation in fat and liver cells [43]. Therefore, inhibition of InsR interaction with IRS proteins by SOCS-3 and the dephosphorylation of InsR by PTP1B and TCPTP would greatly diminish all downstream signaling, not the least of which is K_{ATP} channel opening, in agreement with the findings from Dodd *et al.* [26, 27]. The sex-specific increase in *Socs3, Ptpn1* and *Ptpn2* mRNA expression with DIO would explain the selective insulin resistance in male versus female NPY/AgRP neurons. By attenuating the *Socs3, Ptpn1* and *Ptpn2* expression in DIO females, E_2 preserved the ability of insulin to hyperpolarize NPY/AgRP neurons via K_{ATP} channel opening. E_2 also maintains the efficacy of insulin to depolarize and excite POMC neurons in DIO females, which complements the anorexigenic actions of E_2 in NPY/AgRP neurons [11]. Likewise, a recent paper from Dodd and colleagues has shown that TCPTP plays a critical role in governing the response of POMC neurons to the excitatory effects of insulin such that the phosphatase activity attenuates the insulin response in DIO males [50]. A more recent publication has also implicated PTP1B *(Ptpn1)* in attenuating insulin signaling in NPY/AgRP neurons in hyperleptinemia states [47], and indeed *Ptpn1* mRNA expression was up-regulated in DIO males but not DIO females. As proof of principle, we found that using the non-selective phosphatase inhibitor CX08005 rescued the insulin response in NPY/AgRP neurons from DIO males. Therefore, there is potentially a triad of “negative”

molecular regulators *(Socs3, Ptpn1, Ptpn2)* of insulin receptor coupling in obese states, but inhibiting the phosphatase activity (PTP1B and TCPTP) appears to be sufficient to restore the insulin response in DIO males (current findings).

In obese male mice, hypothalamic levels of *Ptpn2* mRNA and TCPTP are high and remain elevated even after feeding (present results) [26, 51], and the resultant sustained repression of insulin receptor signaling in NPY/AgRP neurons most probably contributes to the elevated hepatic glucose production and hyperglycemia characteristic of the obese and insulin-resistant state. Feeding- and fasting-associated fluctuations of TCPTP protein in NPY/AgRP neurons help coordinate hepatic glucose production such that *icv* insulin is ineffective to alter hepatic function in food-restricted control male mice, whose hypothalamic TCPTP levels are elevated [26]. However, *Ptpn2* deletion in NPY/AgRP neurons can reinstate the response to *icv* insulin. Enhancement of insulin inhibition of NPY/AgRP neurons by *Ptpn2* deletion in males also improves glucose metabolism through the promotion of brown and beige adipose tissue glucose uptake [26, 52]. In fed/satiated male mice in which TCPTP is down-regulated, the resultant enhancement of insulin signaling and resultant inhibition of NPY/AgRP neurons increases sympathetic activity and browning of white adipose tissue to promote the expenditure of energy. Therefore, the results from multiple labs [9, 16–18, 26, 27] support a critical role of insulin signaling in NPY/AgRP neurons to coordinate hepatic glucose production with whole body metabolism to prevent hypoglycemia in fasted states. However, more studies are needed in female mice to determine if there are sex differences in control of hepatic glucose production.

We can state with some certainty that circulating estrogens are responsible for the sex difference in protecting females against insulin resistance in the obese state since we restored insulin signaling in ovariectomized females with EB replacement therapy (present findings and [11]). An obvious question is what is the mechanism(s) by which E_2 protects hypothalamic neurons against insulin resistance? Complementary to its physiological actions in NPY/AgRP neurons, the anorexigenic hormone E_2 also protects female POMC neurons against insulin resistance in the obese state. In POMC neurons however, insulin (and leptin) activate TRPC5 channels, and E_2 preserves the ability of insulin to activate TRPC5 channels and depolarize POMC neurons in obese female mice [11]. Similar to NPY/AgRP neurons, the insulin response in POMC neurons was abrogated in ovariectomized, DIO females but restored with E_2 replacement *(i.e.*, EB treatment). Besides its direct excitatory effects on POMC neurons [53–57], the longer term protective actions of E_2 in POMC neurons are due to alterations in several key genes [11]. Prominently, E_2 up-regulates *Cav3.1* mRNA expression and the T-type calcium current that collaborates with TRPC5 channels to drive Ca^{2+} currents in POMC neurons. On the other hand, E_2 inhibits the expression of endosomal membrane protein stromal-interaction molecule1 *(Stim1)*, which is responsible for sequestering TRPC5 channels from plasma membrane receptor activation [11]. Under normal physiological conditions, TRPC5 channel complexes are coupled to plasma membrane receptors (InsR, leptin receptor and G protein-coupled receptors like serotonin $5HT_{2c}$) in POMC neurons but in stressed states such as with obesity, the TRPC5 channels associate with STIM1 and become coupled to calcium store regulation within the endoplasmic reticulum [58]. Moreover similar to NPY/AgRP neurons, E_2 prevents the increase in SOCS-3 (*Socs3* mRNA) expression in POMC neurons of DIO females. Most of

these transcriptional effects of E_2 in POMC neurons are thought to be mediated by an estrogen receptor α (ERα)-dependent mechanism since ovariectomy leads to hyperphagia [59–61], which is recapitulated by selective deletion of ERα in POMC neurons [62]. However, NPY/AgRP neurons are not thought to express the transcription factors ERα and ERβ [63], although we have documented the mRNA expression of ERα in NPY/AgRP neurons [64]. In addition, we have discovered that there are other non-classical estrogenic signaling mechanisms in NPY/AgRP neurons [35]. Moreover, in NPY/AgRP neurons we have identified a number of channels and signaling molecules that are up-regulated by E_2 treatment. Prominent among the channels is the KCNQ5 channel, which underlies the sub-threshold inhibitory M-current [64, 65]. We have also documented non-canonical membrane associated ERα and Gq-coupled membrane associated estrogen receptor (GqMER) signaling pathways in NPY/AgRP neurons [35]. Selective activation of GqMER by STX rapidly inhibits NPY/AgRP neurons, which correlates with the reduced food intake and weight gain in STX-treated, gonadectomized mice and guinea pigs [35, 57]; and long-term treatment (4 weeks) with STX downregulates the expression of NPY, which correlates with its inhibitory actions on feeding and weight gain after ovariectomy [57, 66].

Besides the pronounced effects of non-canonical E_2 signaling on the endogenous excitability of NPY/AgRP neurons, the steroid hormone E2 also augments inhibitory synaptic input, specifically the inhibitory glutamatergic (mGluR7-mediated) input from kisspeptin neurons [38] and μ-opioid input from POMC neurons [67]. Furthermore, STX enhances $G\alpha_{i,o}$-coupled receptor *(e.g.*, GABAb, mGluR7 and μ-opioid)-mediated activation of G protein-coupled inwardly rectifying K^+ channels [35]. Therefore, E2 inhibits NPY/AgRP neurons using multiple signaling pathways to preserve insulin signaling under physiological and pathophysiological (*i.e.*, obesity) conditions, which underscores the physiological importance of this gonadal steroid. Although testosterone is aromatized to E_2 in the hypothalamus [68], there appears not to be enough conversion of testosterone to preserve insulin signaling in the obese male. However, we have found that similar to females the selective GqMER ligand STX can reduce food intake and weight gain in males [35], which argues for an estrogenic protective signaling pathway in the NPY/AgRP neurons in males. Future experiments need to address this possibility, but clearly our results have identified a vital role for E2 in preserving insulin receptor coupling to channel activation in NPY/AgRP and POMC neurons and thus protect against the development of insulin resistance in obese females.

Acknowledgements

Funding Sources: This work was supported by US National Institutes of Health Grants NS038809 (to M.J.K.), NS043330 (to O.K.R.) and DK068098 (to M.J.K. and O.K.R.).

References

1. Gao Q, Horvath TL: Neurobiology of feeding and energy expenditure. Annu Rev Neurosci 2007;30:367–398. [PubMed: 17506645]
2. Chen Y, Knight ZA: Making sense of the sensory regulation of hunger neurons. BioEssays 2016;38:316–324 [PubMed: 26898524]
3. Aponte Y, Atasoy D, Sternson SM: AGRP neurons are sufficient to orchestrate feeding behavior rapidly and without training. Nat Neurosci 2011;14:351–355 [PubMed: 21209617]

4. Krashes MJ, Koda S, Ye C, Rogan SC, Adams AC, Cusher DS, Maratos-Flier E, Roth BL, Lowell BB: Rapid, reversible activation of AgRP neurons drives feeding behavior in mice. J Clin Invest 2011;121:1424–1428. [PubMed: 21364278]
5. Wei Q, Krolewski DM, Moore S, Kumar V, Li F, Martin B, Tomer R, Murphy GG, Deisseroth K, Watson SJ, Akil H: Uneven balance of power between hypothalamic peptidergic neurons in the control of feeding. Proc Natl Acad Sci USA 2018;115:E9489–E9498. [PubMed: 30224492]
6. Schwartz MW, Woods SC, Porte D Jr., Seeley RJ, Baskin DG: Central nervous system control of food intake. Nature 2000;404:661–671. [PubMed: 10766253]
7. Morton GJ, Cummings DE, Baskin DG, Barsh GS, Schwartz MW: Central nervous system control of food intake and body weight. Nature 2006;443:289–295. [PubMed: 16988703]
8. Belgardt BF, Bruning JC: CNS leptin and insulin action in the control of energy homeostasis. Ann N Y Acad Sci 2010;1212:97–113. [PubMed: 21070248]
9. Qiu J, Zhang C, Borgquist A, Nestor CC, Smith AW, Bosch MA, Ku S, Wagner EJ, Rønnekleiv OK, Kelly MJ: Insulin excites anorexigenic proopiomelanocortin neurons via activation of canonical transient receptor potential channels. Cell Metab 2014;19:682–693. [PubMed: 24703699]
10. Ruud J, Steculorum SM, Brüning JC: Neuronal control of peripheral insulin sensitivity and glucose metabolism. Nat Commun 2017;8:15259. [PubMed: 28469281]
11. Qiu J, Bosch MA, Meza C, Navarro UV, Nestor CC, Wagner EJ, Rønnekleiv OK, Kelly MJ: Estradiol protects proopiomelanocortin neurons against insulin resistance. Endocrinology 2018;159:647–664. [PubMed: 29165691]
12. Benoit SC, Air EL, Coolen LM, Strauss R, Jackman A, Clegg DJ, Seeley RJ, Woods SC: The catabolic action of insulin in the brain is mediated by melanocortins. J Neurosci 2002;22:9048–9052. [PubMed: 12388611]
13. Brown LM, Clegg DJ, Benoit SC, Woods SC: Intraventricular insulin and leptin reduce food intake and body weight in C57BL/6J mice. Physiol Behav 2006;89:687–691. [PubMed: 16979194]
14. Clegg DJ, Gotoh K, Kemp C, Wortman MD, Benoit SC, Brown LM, D'Alessio D,Tso P, Seeley RJ, Woods SC: Consumption of a high-fat diet induces central insulin resistance independent of adiposity. Physiol Behav 2011;103:10–16. [PubMed: 21241723]
15. Obici S, Zhang BB, Karkanias G, Rossetti L: Hypothalamic insulin signaling is required for inhibition of glucose production. Nat Med 2002;8:1376–1382. [PubMed: 12426561]
16. Könner AC, Janoschek R, Plum L, Jordan SD, Rother E, Ma X, Xu C, Enriori P, Hampel B, Barsh GS, Kahn CR, Cowley MA, Ashcroft FM, Brüning JC: Insulin action in AgRP-expressing neurons is required for suppression of hepatic glucose production. Cell Metab 2007;5:438–449. [PubMed: 17550779]
17. Lin HV, Plum L, Ono H, Gutierrez-Juarez R, Shanabrough M, Borok E, Horvath TL, Rossetti L, Accili D: Divergent regulation of energy expenditure and hepatic glucose production by insulin receptor in agouti-related protein and POMC neurons. Diabetes 2010;59:337–346. [PubMed: 19933998]
18. Scherer T, O'Hare J, Diggs-Andrews K, Schweiger M, Cheng B, Lindtner C, Zielinski E, Vempati P, Su K, Dighe S, Milsom T, Puchowicz M, Scheja L, Zechner R, Fisher SJ, Previs SF, Buettner C: Brain insulin controls adipose tissue lipolysis and lipogenesis. Cell Metab 2011;13:183–194. [PubMed: 21284985]
19. Spanswick D, Smith MA, Mirshamsi S, Routh VH, Ashford ML: Insulin activates ATP-sensitive K^+ channels in hypothalamic neurons of lean, but not obese rats. Nat Neurosci 2000;3:757–758. [PubMed: 10903566]
20. Plum L, Rother E, Munzberg H, Wunderlich FT, Morgan DA, Hampel B, Shanabrough M, Janoschek R, Konner AC, Alber J, Suzuki A, Krone W, Horvath TL, Rahmouni K, Bruning JC: Enhanced leptin-stimulated Pi3k activation in the CNS promotes white adipose tissue transdifferentiation. Cell Metab 2007;6:431–445. [PubMed: 18054313]
21. Huang Y, He Z, Gao Y, Lieu L, Yao T, Sun J, Liu T, Javadi C, Box M, Afrin S, Guo H, Williams KW: Phosphoinositide 3-kinase is integral for the acute activity of leptin and insulin in male arcuate NPY/AgRP neurons. J Endocrine Soc 2018;2:518–532 [PubMed: 29850651]

22. Rameh LE, Rhee SG, Spokes K, Kazlauskas A, Cantley LC, Cantley LG: Phosphoinositide 3-kinase regulates phospholipase Cγ-mediated calcium signaling. J Biol Chem 1998;273:23750–23757. [PubMed: 9726983]
23. Falasca M, Logan SK, Lehto VP, Baccante G, Lemmon MA, Schlessinger J: Activation of phospholipase Cy by PI 3-kinase-induced PH domain-mediated membrane targeting. EMBO J 1998;17:414–422. [PubMed: 9430633]
24. Bae YS, Cantley LG, Chen C-S, Kim S-R, Kwon K-S, Rhee SG: Activation of phospholipase C-γ by phosphatidylinositol 3,4,5-trisphosphate. J Biol Chem 1998;273:4465–4469. [PubMed: 9468499]
25. Shyng S-L, Nichols CG: Membrane phospholipid control of nucleotide sensitivity of K_{ATP} channels. Science 1998;282:1138–1141. [PubMed: 9804554]
26. Dodd GT, Andrews ZB, Simonds SE, Michael NJ, DeVeer M, Brüning JC, Spanswick D, Cowley MA, Tiganis T: A hypothalamic phosphatase switch coordinates energy expenditure with feeding. Cell Metab 2017;26:577. [PubMed: 28877462]
27. Dodd GT, Lee-Young RS, Brüning JC, Tiganis T: TCPTP regulates insulin signalling in AgRP neurons to coordinate glucose metabolism with feeding. Diabetes 2018;67:1246–1257. [PubMed: 29712668]
28. Pocai A, Lam TKT, Guiterrez-Juarez R, Obici S, Schwartz GJ, Bryan J, Aguilar-Bryan L, Rossetti L: Hypothalamic K_{ATP} channels control hepatic glucose production. Nature 2005;434:1026–1031. [PubMed: 15846348]
29. Kim B, Feldman EL: Insulin resistance in the nervous system. Trends Endocrinol Metabl 2012;23:133–141.
30. Janssen I, Powell LH, Crawford S, Lasley B, Sutton-Tyrrell K: Menopause and the metabolic syndrome: the Study of Women's Health Across the Nation. Arch Intern Med 2008;168:1568–1575. [PubMed: 18663170]
31. Gustafsson PE, Persson M, Hammarstrom A: Life course origins of the metabolic syndrome in middle-aged women and men: the role of socioeconomic status and metabolic risk factors in adolescence and early adulthood. Ann Epidemiol 2011;21:103–110. [PubMed: 21184951]
32. Van den Pol AN, Yao Y, Fu L-Y, Foo K, Huang H, Coppari R, Lowell BB, Broberger C: Neuromedin B and gastrin-releasing peptide excite arcuate nucleus neuropeptide Y neurons in a novel transgenic mouse expressing stong *renilla* green fluorescent protein in NPY neurons. J Neurosci 2009;29:4622–4639. [PubMed: 19357287]
33. Parton LE, Ye CP, Coppari R, Enriori PJ, Choi B, Zhang C-Y, Xu C, Vianna CR, Lee CE, Elmquist JK, Cowley MA, Lowell BB: Glucose sensing by POMC neurons regulates glucose homeostasis and is impaired in obesity. Nature 2007;449:228–232. [PubMed: 17728716]
34. Paeger L, Pippow A, Hess S, Paehler M, Klein AC, Husch A, Pouzat C, Bruning JC, Kloppenburg P: Energy imbalance alters Ca^{2+} handling and excitability of POMC neurons. eLife 2017;6:1–21.
35. Smith AW, Bosch MA, Wagner EJ, Rønnekleiv OK, Kelly MJ: The membrane estrogen receptor ligand STX rapidly enhances GABAergic signaling in NPY/AgRP neurons: Role in mediating the anorexigenic effects of 17β-estradiol. Am J Physiol Endo Metab 2013;305:E632–E640.
36. Zhang C, Tonsfeldt KJ, Qiu J, Bosch MA, Kobayashi K, Steiner RA, Kelly MJ, Rønnekleiv OK: Molecular mechanisms that drive estradiol-dependent burst firing of Kiss1 neurons in the rostral periventricular preoptic area. Am J Physiol Endo Metab 2013;305:E1384–E1397.
37. Bosch MA, Tonsfeldt KJ, Rønnekleiv OK: mRNA expression of ion channels in GnRH neurons: subtype-specific regulation by 17β-Estradiol. Mol Cell Endocrinol 2013;367:85–97. [PubMed: 23305677]
38. Qiu J, Rivera HM, Bosch MA, Padilla SL, Stincic TL, Palmiter RD, Kelly MJ, Rønnekleiv OK: Estrogenic-dependent glutamatergic neurotransmission from kisspeptin neurons governs feeding circuits in females. eLife 2018;7:e35656. [PubMed: 30079889]
39. Zhang C, Bosch MA, Rønnekleiv OK, Kelly MJ: 17β-estradiol increases persistent Na^+ current and excitability of AVPV/PeN Kiss1 neurons in female mice. Mol Endocrinol 2015;29:518–527. [PubMed: 25734516]
40. Pfaffl MW: A new mathematical model for relative quantification in real-time RT PCR. Nucleic Acids Res 2001;29:e45. [PubMed: 11328886]

41. Schmittgen TD, Livak KJ: Analyzing real-time PCR data by the comparative C_T method. Nat Protoc 2008;3:1101–1108. [PubMed: 18546601]
42. Ashcroft FM, Gribble FM: New windows on the mechanism of action of K^{ATP} channel openers. Trends Pharmacol Sci 2000;21:439–445. [PubMed: 11121575]
43. Howard JK, Flier JS: Attenuation of leptin and insulin signaling by SOCS proteins. Trends Endocrinol Metab 2006;17:365–371. [PubMed: 17010638]
44. Kievit P, Howard JK, Badman MK, Balthasar N, Coppari R, Mori H, Lee CE, Elmquist JK, Yoshimura A, Flier JS: Enhanced leptin sensitivity and improved glucose homeostasis in mice lacking suppressor of cytokine signaling-3 in POMC-expressing cells. Cell Metab 2006;4:123–132 [PubMed: 16890540]
45. Zhang Z-Y, Dodd GT, Tiganis T: Protein tyrosine phosphatases in hypothalamic insulin and leptin signaling. Trends Pharmacol Sci 2015;36:661–674 [PubMed: 26435211]
46. Al-Qassab H, Smith MA, Irvine EE, Guillermet-Guibert J, Claret M, Choudhury AI,Selman C, Piipari K, Clements M, Lingard S, Chandarana K, Bell JD, Barsh GS, Smith AJH, Batterham RL, Ashford MLJ, Vanhaesebroeck B, Withers DJ: Dominant role of the p110β isoform of PI3K over p110α in energy homeostasis regulation by POMC and AgRP neurons. Cell Metab 2009;10:343–354. [PubMed: 19883613]
47. Balland E, Chen W, Dodd GT, Conductier G, Coppari R, Tiganis T, Cowley MA: Leptin signaling in the arcuate nucleus reduces insulin's capacity to suppress hepatic glucose production in obese mice. Cell Rep 2019;26:346–355.e343. [PubMed: 30625317]
48. Zhang X, Tian J, Li J, Huang L, Wu S, Liang W, Zhong L, Ye J, Ye F: A novel protein tyrosine phosphatase 1B inhibitor with therapeutic potential for insulin resistance. Br J Pharmacol 2016;173:1939–1949. [PubMed: 26990621]
49. Pedroso JAB, Buonfiglio DC, Cardinali LI, Furigo IC, Ramos-Lobo AM, Tirapequi J, Elias CF, Donato J Jr.: Inactivation of SOCS3 in leptin receptor-expressing cells protects mice from diet-induced insulin resistance but does not prevent obesity. Mol Metab 2014;3:608–618. [PubMed: 25161884]
50. Dodd GT, Michael NJ, Lee-Young RS, Mangiafico SP, Pryor JT, Munder AC, Simonds SE, Brüning JC, Zhang Z-Y, Cowley MA, Andrikopoulos S, Horvath TL, Spanswick D, Tiganis T: Insulin regulates POMC neuronal plasticity to control glucose metabolism. eLife 2018;7:e38704. [PubMed: 30230471]
51. Loh K, Fukushima A, Zhang X, Galic S, Briggs D, Enriori Pablo J, Simonds S, Wiede F, Reichenbach A, Hauser C, Sims Natalie A, Bence Kendra K, Zhang S, Zhang Z-Y, Kahn Barbara B, Neel Benjamin G, Andrews Zane B, Cowley Michael A, Tiganis T: Elevated hypothalamic TCPTP in obesity contributes to cellular leptin resistance. Cell Metab 2011;14:684–699. [PubMed: 22000926]
52. Dodd GT, Decherf S, Loh K, Simonds SE, Wiede F, Balland E, Merry TL, Munzberg H, Zhang ZY, Kahn BB, Neel BG, Bence KK, Andrews ZB, Cowley MA, Tiganis T: Leptin and insulin act on POMC neurons to promote the browning of white fat. Cell 2015;160:88–104. [PubMed: 25594176]
53. Kelly MJ, Loose MD, Rønnekleiv OK: Estrogen suppresses μ-opioid and GABAb-mediated hyperpolarization of hypothalamic arcuate neurons. J Neurosci 1992;12:2745–2750. [PubMed: 1319480]
54. Lagrange AH, Rønnekleiv OK, Kelly MJ: The potency of μ-opioid hyperpolarization of hypothalamic arcuate neurons is rapidly attenuated by 17β-estradiol. J Neurosci 1994;14:6196–6204. [PubMed: 7931572]
55. Lagrange AH, Rønnekleiv OK, Kelly MJ: Modulation of G protein-coupled receptors by an estrogen receptor that activates protein kinase A. Mol Pharmacol 1997;51:605–612. [PubMed: 9106625]
56. Qiu J, Bosch MA, Tobias SC, Grandy DK, Scanlan TS, Rønnekleiv OK, Kelly MJ: Rapid signaling of estrogen in hypothalamic neurons involves a novel G-protein-coupled estrogen receptor that activates protein kinase C. J Neurosci 2003;23:9529–9540. [PubMed: 14573532]

57. Qiu J, Bosch MA, Tobias SC, Krust A, Graham S, Murphy S, Korach KS, Chambon P, Scanlan TS, Rønnekleiv OK, Kelly MJ: A G-protein-coupled estrogen receptor is involved in hypothalamic control of energy homeostasis. J Neurosci 2006;26:5649–5655. [PubMed: 16723521]
58. Arruda AP, Pers BM, Parlakgul G, Guney E, Goh T, Cagampan E, Lee GY, Goncalves RL, Hotamisligil GS: Defective STIM-mediated store operated Ca^{2+} entry in hepatocytes leads to metabolic dysfunction in obesity. eLife 2017;6:e29968. [PubMed: 29243589]
59. Ahdieh HB, Wade GN: Effects of hysterectomy on sexual receptivity, food intake, running wheel activity, and hypothalamic estrogen and progestin receptors in rats. J Comp Physiol Psychol 1982;96:886–892 [PubMed: 7153386]
60. Geary N: Estradiol and the control of eating. Appetite 1997;29:386. [PubMed: 9468768]
61. Eckel LA: Estradiol: a rhythmic, inhibitory, indirect control of meal size. Physiol Behav 2004;82:35–41. [PubMed: 15234587]
62. Xu Y, Nedungadi TP, Zhu L, Sobhani N, Irani BG, Davis KE, Zhang X, Zou F, Gent LM, Hahner LD, Khan SA, Elias CF, Elmquist JK, Clegg DJ: Distinct hypothalamic neurons mediate estrogenic effects on energy homeostasis and reproduction. Cell Metab 2011;14:453–465. [PubMed: 21982706]
63. Olofsson LE, Pierce AA, Xu AW: Functional requirement of AgRP and NPY neurons in ovarian cycle-dependent regulation of food intake. Proc Natl Acad Sci USA 2009;106:15932–15937. [PubMed: 19805233]
64. Roepke TA, Qiu J, Smith AW, Rønnekleiv OK, Kelly MJ: Fasting and 17β-estradiol differentially modulate the M-current in neuropeptide Y neurons. J Neurosci 2011;17:11825–11835.
65. Roepke TA, Malyala A, Bosch MA, Kelly MJ, Rønnekleiv OK: Estrogen regulation of genes important for K+ channel signaling in the arcuate nucleus. Endocrinology 2007;148:4937–4951. [PubMed: 17595223]
66. Roepke TA, Xue C, Bosch MA, Scanlan TS, Kelly MJ, Rønnekleiv OK: Genes associated with membrane-initiated signaling of estrogen and energy homeostasis. Endocrinology 2008;149:6113–6124 [PubMed: 18755790]
67. Stincic TL, Rønnekleiv OK, Kelly MJ: Diverse actions of estradiol on anorexigenic and orexigenic hypothalamic arcuate neurons. Horm Behav 2018;104:146–155. [PubMed: 29626486]
68. Roselli CE, Resko JA: The distribution and regulation of aromatase activity in the central nervous system. Steroids 1987;50:495–508. [PubMed: 3332938]

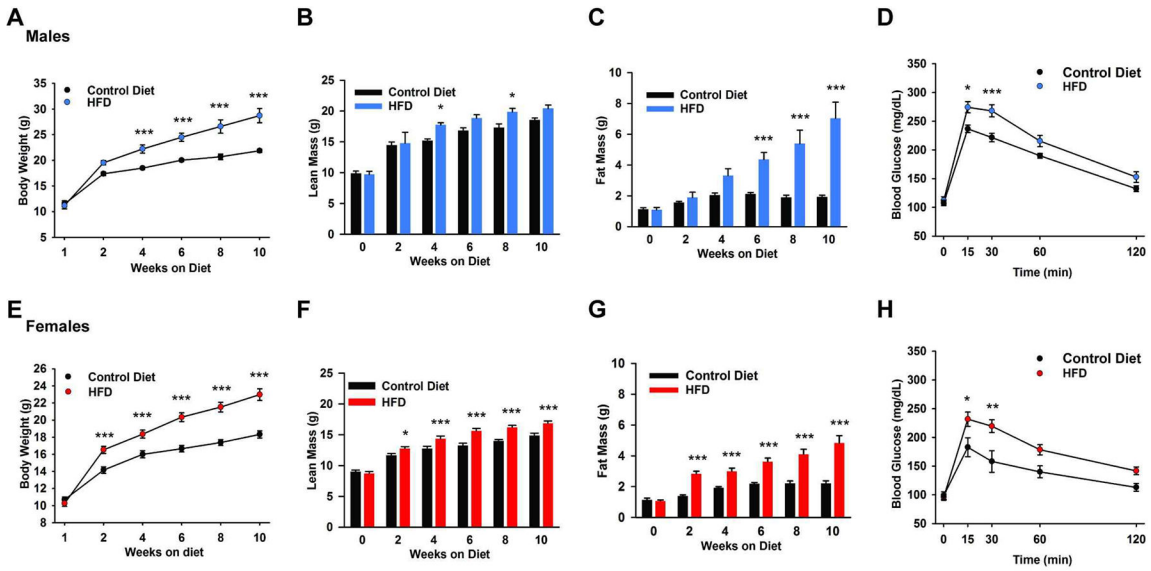

Fig. 1. Male and female mice on high fat diet become obese and glucose intolerant.

A,B,C, Male *Npy*^{GFP} mice were maintained on a high fat diet (45% fat) or a control, grain based diet for 10 weeks. The high fat diet caused a significant weight gain and diet induced obesity (DIO) (**A**) over the 10 week period which was significantly different from controls by week 4 (two-way ANOVA: main effect of treatment ($F_{(1,42)}$ = 66.10, p < 0.001), main effect of time ($F_{(5,42)}$ = 75.43, p < 0.001) and interaction ($F_{(5,42)}$ = 5.151, p = 0.001); Control n = 4, DIO mice n = 5; *post hoc* Bonferroni test). **B** and **C**, lean mass and total body fat were measured by EchoMRI. Lean mass (B) does not include bone and fluids within organs. The difference in fat content (C) between the groups became significantly different at six weeks. Two-way ANOVA for B: main effect of treatment ($F_{(1,42)}$ =12.36, p = 0.001), main effect of time ($F_{(5,42)}$ =44.13, p < 0.001) and interaction ($F_{(5,42)}$ = 1.191, p = 0.3299); Control mice n = 4; DIO mice n = 5; *post hoc* Bonferroni test; Two-way ANOVA for C: main effect of treatment $F_{(1,42)}$ = 48.82, p < 0.001, main effect of time $F_{(5,42)}$ = 11.72, p < 0.001, and interaction ($F_{(5,42)}$ = 7.359, p < 0.001). Control mice n = 4, DIO mice n = 5; *post hoc* Bonferroni tests). **E, F, G** Female *Npy*^{GFP} mice were maintained on a high fat diet (45% fat) or a control, grain based diet for 10 weeks. The high fat diet caused a significant weight gain and diet-induced obesity (E) over the 10 week period, which was significantly different than controls by week 2 (two-way ANOVA: main effect of treatment ($F_{(1,108)}$ = 95.54, p < 0.001), main effect of time ($F_{(5,108)}$ = 108.7, p < 0.001) and interaction ($F_{(5,108)}$ = 6.819, p < 0.001); Control-diet n = 8, DIO mice n = 12; *post hoc* Bonferroni test). **F** and **G**, the lean (F) and fat (G) content between groups became significantly different at two weeks (two-way ANOVA for the lean mass (F): main effect of treatment ($F_{(1, 108)}$ = 51.31, p < 0.001), main effect of time ($F_{(5,108)}$ = 97.79, p < 0.001) and interaction ($F_{(5,108)}$ = 3.606, p = 0.005), Control mice n = 8; DIO mice n = 12; Two-way ANOVA for fat content mass (G): main effect of treatment ($F_{(1,108)}$ = 93.75, p < 0.001), main effect of time ($F_{(5,108)}$ = 23.74, p < 0.001) and interaction ($F_{(5,108)}$ = 6.426, p < 0.001), Control mice n = 8; DIO mice n = 12; *post hoc* Bonferroni tests). *p < 0.05; ***p < 0.005. Both (**D**) DIO male and (**H**) female *NPY*^{GFP} mice at 10 weeks exhibited glucose intolerance vs their age-matched controls (fed grain-based diet). The GTTs showed significantly higher peak blood glucose levels 15

minutes after *i.p.* glucose (see “Materials and Methods”) and a delayed clearance. Two-way ANOVA for D: main effect of treatment ($F_{(1,95)}$ = 25.48, p < 0.0001), main effect of time ($F_{(4,95)}$ = 114.5, p < 0.0001) and interaction ($F_{(4,95)}$ =1.862, p = 0.1234); control, n = 9, HFD, n = 12; *post hoc* Bonferroni test, *p < 0.05; ***p <0.005. Two-way ANOVA for H: main effect of treatment ($F_{(1,85)}$ =20.76, p < 0.0001), main effect of time ($F_{(4,85)}$ = 25.55, p < 0.0001) and interaction ($F_{(4,85)}$ = 1.775, p = 0.1414); control, n = 8, HFD, n = 12; *post hoc* Bonferroni test, *p < 0.05; **p < 0.01.

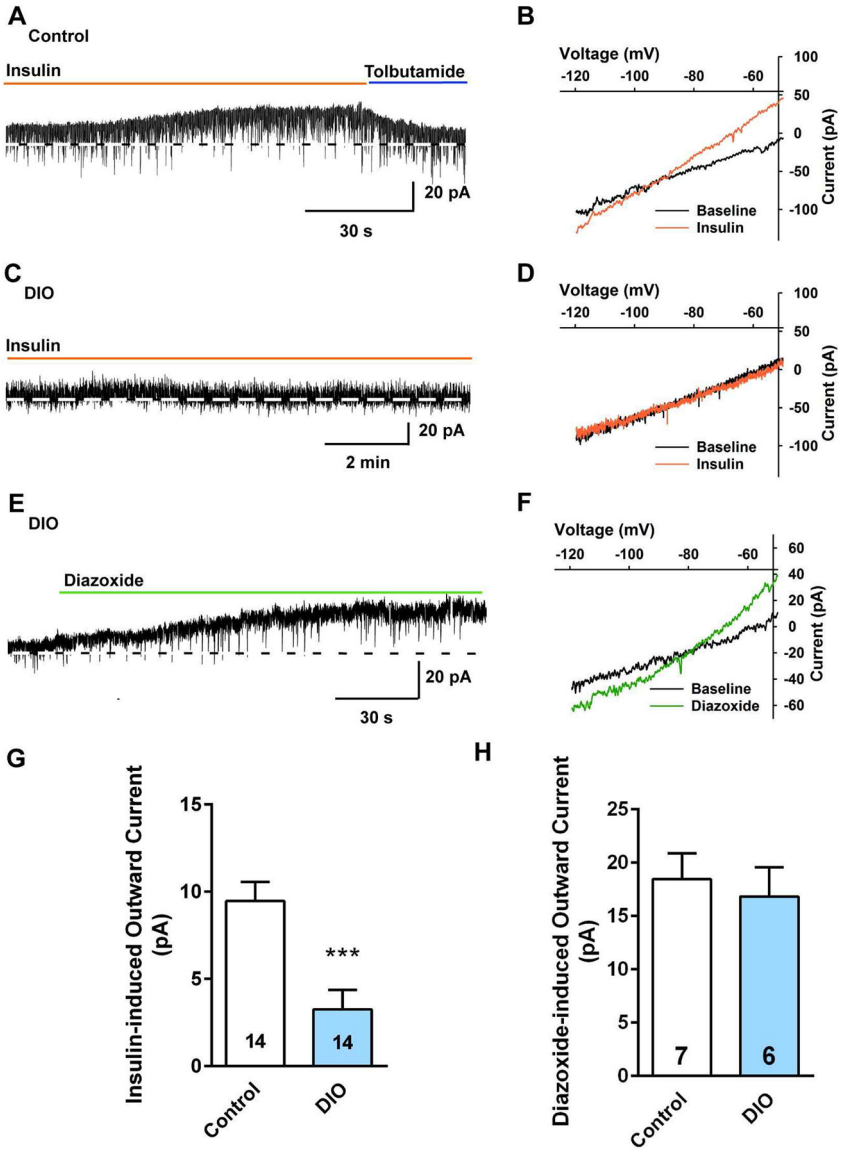

Fig. 2. NPY/AgRP neurons from DIO males are insulin resistant.

In voltage clamp, insulin (20 nM) induced an outward current in NPY/AgRP neurons from male mice on a control diet, which was reversed by the K_{ATP} channel blocker tolbutamide (100 μM) (**A**), but had no effect in NPY/AgRP neurons from DIO male mice (**C**). V_{hold} = −60 mV. **B**, the I-V relationship for the insulin-induced current from a control diet-fed mouse was obtained from the recording in A showing an outward current which had a reversal potential close to E_{k+} (−87.7 ± 4.3 mV, n = 3). **D**, the I-V relationship for the insulin-induced current from a DIO mouse obtained from the recording in C showed no evidence of an increased K^+ conductance with bath perfusion of insulin. **E**, K_{ATP} channel opener diazoxide (300 μM) induced an outward K^+ current in NPY/AgRP neurons from DIO males that did not respond to insulin. **F**, the I-V relationship obtained from the recording in E showing an outward current which had a reversal potential close to E_{k+} (−90 ± 2.6 mV, n = 6). **G** and **H**, Bar graphs summarizing the insulin- (G) and diazoxide-induced (H) outward

currents in NPY/AgRP neurons from control diet, and DIO male mice. Data points represent the mean ± SEM. Un-paired *t*-test for G: $t_{(26)} = 3.989$, $p = 0.0005$; ***$p < 0.005$ versus control; un-paired *t*-test for H: $t_{(11)} = 0.4438$, $p = 0.6658$. Cell numbers are indicated.

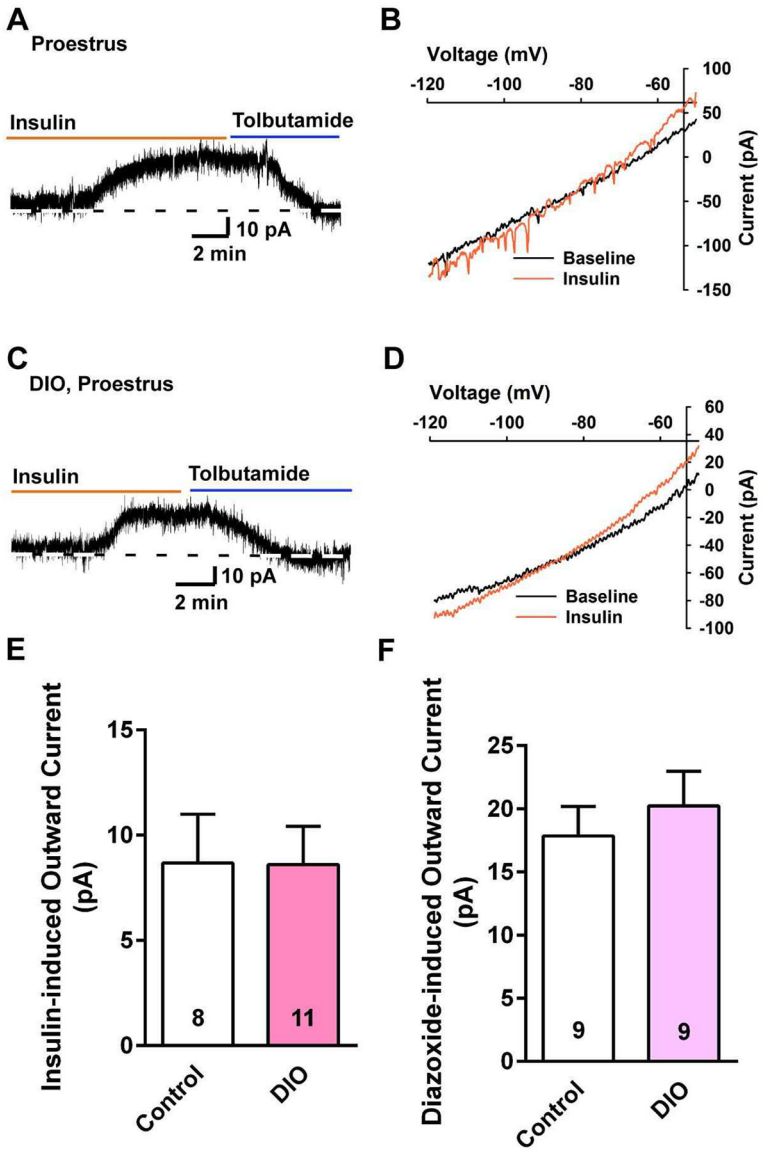

Fig. 3. NPY/AgRP neurons from DIO, proestrous females are protected against insulin resistance.

A and C, in voltage clamp, insulin (20 nM) induced outward currents in NPY/AgRP neurons from proestrous female mice on a control diet (A) or DIO female mice (C), both of which were antagonized by tolbutamide. V_{hold} = − 60 mV. Tolbutamide was equally efficacious to reverse the effects of insulin in control and DIO females (control: 14.6 ± 3.2 pA, n = 4; DIO females: 14.7 ± 2.8 pA, n = 6). **B**, the I-V relationship for the insulin-induced current was obtained from the recording in A, which showed an outward current that reversed at E_{k+} (−88.6 ± 1.9 mV, n = 7). **D**, the I-V relationship for the insulin-induced current was obtained from a DIO mouse, which also showed an outward current that reversed at E_{k+} (−87.0 ± 3.1 mV, n = 4). **E** and **F**, bar graphs summarizing the insulin- (E) and diazoxide-induced (F) outward currents in NPY/AgRP neurons from control diet and DIO, proestrous female mice. Data points represent the mean ± SEM. Un-paired *t*-test for E:

$t_{(17)} = 0.02586$, $p = 0.9797$; un-paired t-test for F: $t_{(16)} = 0.5213$, $p = 0.6658$. Cell numbers are indicated.

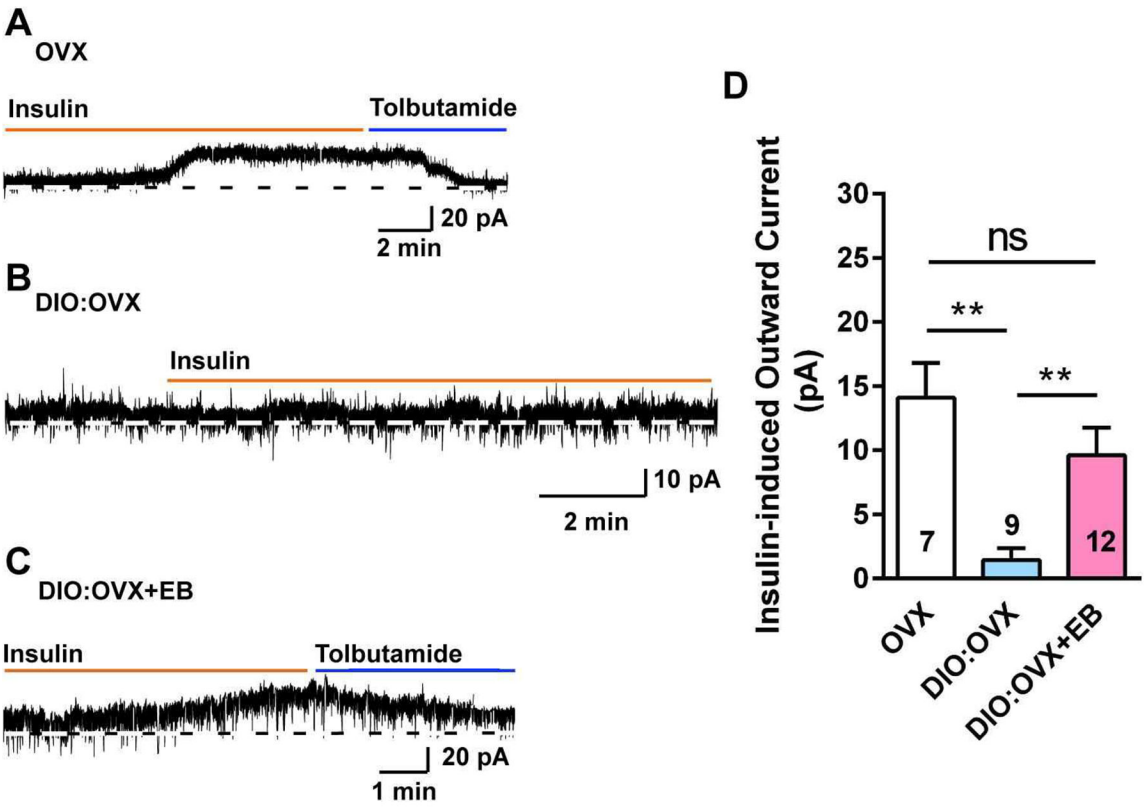

Fig. 4. E_2 replacement rescues insulin response in NPY/AgRP neurons from DIO, ovariectomized females.

A, insulin (20 nM) induced an outward current in voltage clamp in NPY/AgRP neurons from control diet-fed, ovariectomized female mice. The insulin responses were antagonized by K_{ATP} channel blocker tolbutamide. V_{hold} = −60 mV. **B**, in DIO, ovariectomized females, the insulin response was abrogated in NPY/AgRP neurons. **C**, however, the insulin responses in voltage clamp were rescued in DIO, ovariectomized females with EB treatment. **D**, bar graphs summarizing the insulin-induced currents in normal diet and DIO, ovariectomized and E_2-treated female mice. Data points represent the mean ± SEM (control diet, OVX females: 14.1 ± 2.7 pA, n = 7; DIO, OVX females: 1.4 ± 0.9 pA, n = 9; DIO, EB-treated, OVX females: 9.6 ± 2.2 pA, n = 12; one-way ANOVA, effect of treatment, $F_{(2, 25)}$ = 8.531, p = 0.0015; Newman-Keuls' multiple-comparison *post-hoc* test. ** $p < 0.01$; ns, no significant difference). Cell numbers are indicated.

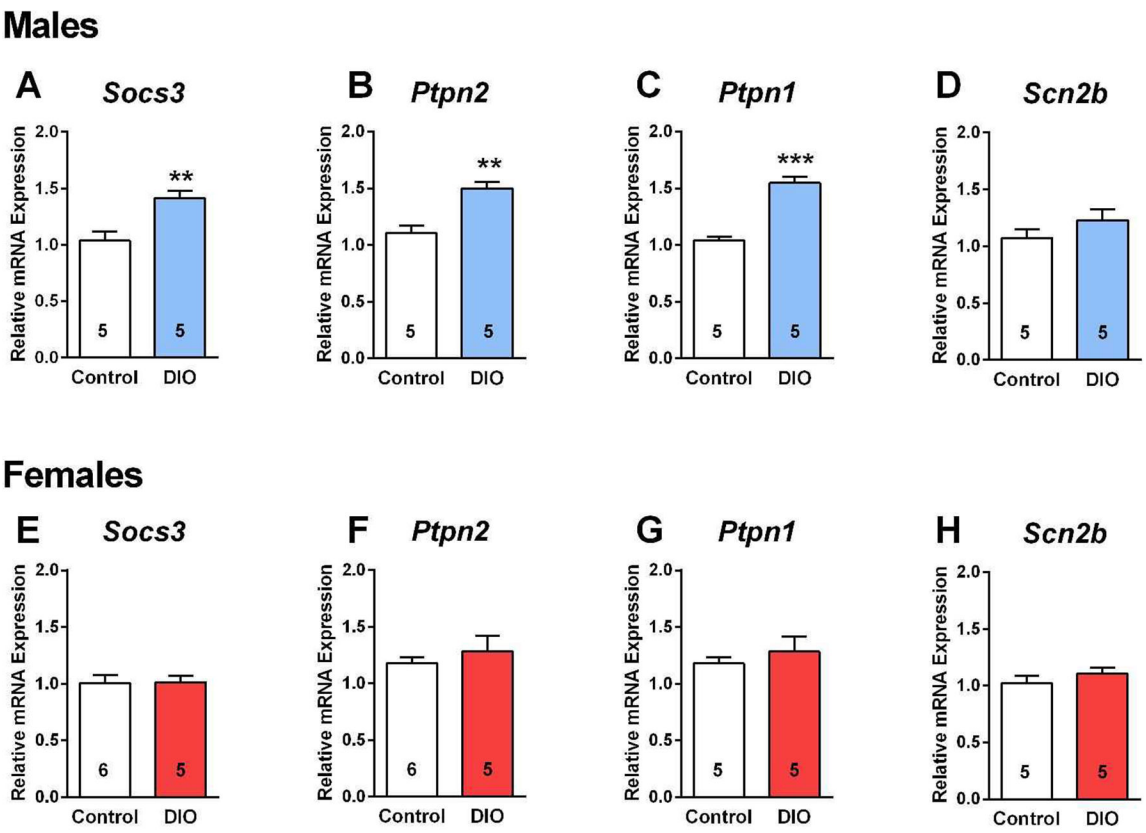

Fig. 5. The mRNA expression levels of *Socs3*, *Ptpn1* and *Ptpn2* are upregulated in NPY/AgRP neurons from male DIO mice.

A-D, HFD consumption led to obesity with corresponding increased mRNA expression of *Socs3, Ptpn2 and Ptpn1, but not Scn2b* in male NPY/AgRP neurons. Un-paired two-tailed *t*-test for A: $t_{(8)} = 3.682$, $p = 0.0062$; Un-paired two-tailed *t*-test for B: $t_{(8)} = 4.703$, $p = 0.0015$; Un-paired two-tailed *t*-test for C: $t_{(8)} = 8.066$, $p < 0.0001$; Un-paired two-tailed *t*-test for D: $t_{(8)} = 1.218$, $p = 0.2362$. **E-H**, none of these genes were significantly increased in NPY/AgRP neurons from OVX + EB treated, DIO females as compared to OVX + EB treated control. Un-paired two-tailed *t*-test for E: $t_{(9)} = 0.0930$, $p = 0.9279$. Un-paired two-tailed *t*-test for F: $t_{(9)} = 0.7574$, p = 0.4682; Un-paired two-tailed *t*-test for G: $t_{(8)} = 0.2648$, $p = 0.7978$; Un-paired two-tailed *t*-test for H: $t_{(8)} = 0.9244$, $p = 0.3823$. Number of animals are indicated. ** $p < 0.01$; *** $p < 0.005$. Data points represents mean ± SEM of relative mRNA expression.

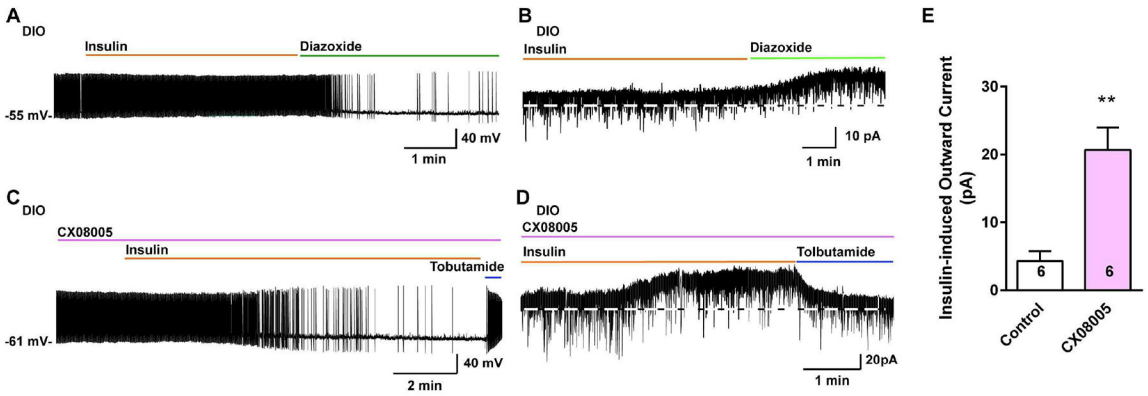

Fig. 6. Insulin–sensitizing effect of CX08005 in NPY/AgRP neurons from male DIO mice.

A, B, insulin (20 nM) did not hyperpolarize and reduce firing in current clamp (A) and induce an outward current in voltage clamp (B), but the K_{ATP} channel opener diazoxide (300 μM) hyperpolarized and induced an outward current in NPY/AgRP neurons from male DIO mice. **C, D**, however after the arcuate slices from DIO males were pretreated with the PTP1B/TCPTP inhibitor CX08055 at 20 μM (treated for 4 hours at 32°C), insulin was fully efficacious to hyperpolarize and inhibit the firing (C) and induce an outward current (D) in NPY/AgRP neurons, and both were antagonized by the K_{ATP} channel blocker tolbutamide (100 μM) V_{hold} = −60 mV. **E**, bar graphs summarizing the insulin-induced currents of NPY/AgRP neurons in control or CX08005 treated arcuate slices from male DIO mice. Data points represent the mean ± SEM. Un-paired *t*-test for D versus B: $t_{(10)} = 4.518$, $p = 0.0011$; ** $p < 0.01$. Cell numbers are indicated. In current clamp, CX08055 also increased the insulin-induced hyperpolarization (CX08055 treated group: −10.0 ± 0.6 mV, n = 2 versus controls: −1.2 ± 0.5 mV, n = 4).

Table 1.

Primer Table

Gene Name (encodes for)	Accession Number	Primer Location (nt)	Product Length (bp)	Annealing Temp (°C)	Efficiency Slope	r^2	%
Socs3 (SOCS3)	NM_007707	1913–1932 2012–2031	119	60	−3.294	0.900	100
Ptpn2 (TCPTP)	NM_008977	404–425 488–509	106	60	−3.305	0.958	100
Ptpn1 (PTP1B)	NM_011201	837–856 908–928	92	60	−3.338	0.955	99
Pik3cb (Pi3Kp110β)	NM_029094	1083–1101 1149–1167	85	60	−3.419	0.970	96
Scn2b (Nav β2)	NM_001014761	187–206 272–291	105	60	−3.356	0.988	99
Gapdh (GAPDH)	NM_008084	689–706 764–781	93	60	−3.352	0.998	99